Audio Engineering Society
Convention Paper

Presented at the 139th Convention
2015 October 29–November 1 New York, USA

Directivity-Customizable Loudspeaker Arrays Using Constant-Beamwidth Transducer (CBT) Overlapped Shading

Xuelei Feng [1], Yong Shen [2], D. B. (Don) Keele, Jr. [3], and Jie Xia [4]

[1, 2, 4] Key Laboratory of Modern Acoustics (Ministry of Education), and Institute of Acoustics, Nanjing University, Nanjing 210093, P. R. China
[1] xlfeng@hotmail.com; [2] yshen@nju.edu.cn; [4] xiajie@nju.edu.cn

[3] DBK Associates and Labs, Bloomington, Indiana 47408, USA
[3] DKeeleJr@Comcast.net

ABSTRACT

In this work, a multiple constant-beamwidth transducer (Multi-CBT) loudspeaker array is proposed, which is constructed by applying multiple overlapping CBT Legendre shadings to a circular-arc or straight-line delay-curved multi-acoustic-source array. Because it has been proved theoretically and experimentally that the CBT array provides constant broadband directivity behavior with nearly no side lobes, the Multi-CBT array can provide a directivity-customizable sound field with frequency-independent element weights by sampling and reconstructing the targeted directivity pattern. Various circularly curved Multi-CBT arrays and straight-line, delay-curved Multi-CBT arrays are analyzed in several application examples that are based on providing constant Sound Pressure Level (SPL) on a seating plane, and their performance capabilities are verified. The power of the method lies in the fact only a few easily-adjustable real-valued element weights completely control the shape of the polar pattern which makes matching the polar shape to a specific seating plane very easy. The results indicate that the desired directivity patterns can indeed be achieved.

1. INTRODUCTION

One important goal of a loudspeaker array is to produce a sound source whose directional characteristics are customizable and constant over a wide frequency band.

1.1. Multi-CBT Source

This paper proposes a variation of the CBT array called the Multi-CBT array that provides adjustability of the coverage pattern by a few simple frequency-independent element weights. The resultant array exhib-

its the superior frequency-independent coverage characteristics and low side lobes of the CBT array but with the added capability of being able to easily adjust its coverage pattern shape without complicated signal-processing devices.

1.2. Previous Methods to Implement Constant-Directivity Arrays

Various methods have been proposed to realize constant-directivity arrays. For example, the Fourier-transform-based arrays [1, 2] can realize extremely constant directivity by using frequency-dependent element weights; additionally, the All-Pass Linear Arrays [3] are omnidirectional over a wide frequency range with frequency-independent element weights. Among these methods, an excellent solution is the use of the constant-beamwidth transducer (CBT), which achieves extremely frequency-independent directivity behavior with frequency-independent element weights, and was provided by U.S. military underwater researchers [4, 5]. Then, Keele applied the CBT theory to loudspeaker arrays, and proposed the circularly curved CBT array [6] and the straight-line, delay-curved CBT array [7]. He also constructed prototype CBT arrays and verified the practical implementation of the CBT loudspeaker arrays experimentally [8, 9].

1.3. Properties of CBT Arrays

Two properties of the CBT array that have been verified theoretically and experimentally are considered in this work: (1) an extremely constant directivity pattern over a wide frequency band, and (2) very low side lobes.

1.4. Properties of Multi-CBT Arrays

This paper shows that it is possible to construct a multiple constant-beamwidth transducer (Multi-CBT) loudspeaker array that can provide the desired directivity behavior by applying a combination of several overlapping CBT Legendre shadings to a circular-arc multi-speaker array, as Fig. 1 shows (usually with overlaps that are typically equal to the half-angles of the individual overlapping Legendre shading functions). Since the directivity pattern of previous CBT arrays has only a single Legendre-function-shaped mainlobe [6], the Multi-CBT array is formed by applying multiple overlapping Legendre shapes to a circular-arc array by sampling and reconstructing the targeted directivity pattern (the mathematical details are described later).

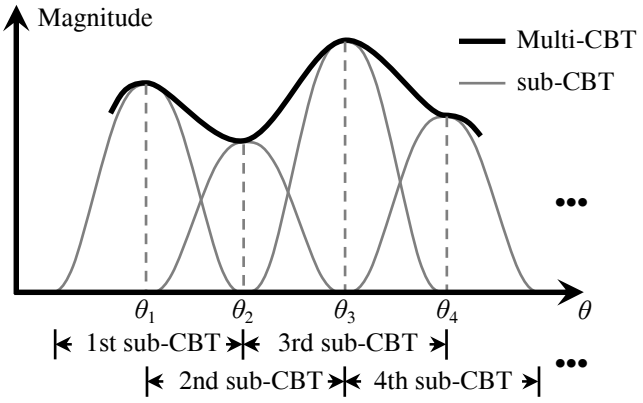

Fig. 1. Polar response of the proposed multiple constant-beamwidth transducer (Multi-CBT) array in the array plane. Several overlapping Legendre shading functions are overlapped at their half-angle points. Weighting functions control the amplitudes of the individual shading functions.

2. THEORY

2.1. Theory of CBT Arrays

The underlying CBT theory is described briefly as follows. If the radial velocity distribution $u(\theta')$ on the surface of a rigid spherical cap conforms to [4]

$$u(\theta') \propto \begin{cases} \mathrm{P}_\nu(\cos\theta'), & \theta' \le \theta_0' \\ 0, & \theta' > \theta_0' \end{cases}, \qquad (1)$$

where $\mathrm{P}_\nu(x)$ is Legendre function of argument x and the order ν $(\nu > 0)$ does not have to be an integer, θ' is the elevation angle in spherical coordinates, θ_0' is the half-angle of the spherical cap and the smallest zero of $\mathrm{P}_\nu(\cos\theta')$ as well, then the far-field sound pressure distribution $p(\theta')$, above a cutoff frequency, is approximated by

$$p(\theta') \propto \begin{cases} \mathrm{P}_\nu(\cos\theta'), & \theta' \le \theta_0' \\ 0, & \theta' > \theta_0' \end{cases}. \qquad (2)$$

This means that the far-field sound pressure distribution is essentially frequency-independent with frequency-independent shading of the driver amplitudes. Furthermore, the CBT theory still works when it is applied to two-dimensional circularly curved arrays [6]. Signal delays can also be used to construct straight-line, delay-curved CBT arrays [7].

2.2. Theory of Multi-CBT Arrays

Since the CBT array has such impressive acoustic properties, the Multi-CBT array can then be constructed by applying several CBT shading functions to a circular-arc un-shaded array to realize the desired directivity pattern. Assuming that the desired directivity pattern is $D(\theta)$, similar to the sampling and reconstruction in the signal-processing field using sinc function, the Multi-CBT array is constructed (see Fig. 1) by using

$$D(\theta) \approx \sum_n D(\theta_n)\,\hat{p}(\theta-\theta_n), \tag{3}$$

where θ is the angle in polar coordinates in the array plane, θ_n is the center angle of the nth sub-CBT array, and $\hat{p}(\theta)$ is the normalized directivity pattern of the sub-CBT array given by:

$$\hat{p}(\theta) = \begin{cases} \mathrm{P}_\nu(\cos\theta), & |\theta| \le \theta_0 \\ 0, & |\theta| > \theta_0 \end{cases}, \tag{4}$$

where θ_0 is the half-angle of the sub-CBT array shading function and the smallest zero of $\mathrm{P}_\nu(\cos\theta)$ as well. Note that the primed angles are in spherical coordinates, whereas the non-primed angles are in polar coordinates in the array plane, that is, because the geometry of the CBT was originally a spherical cap [4, 5], whereas the geometries of the CBT and Multi-CBT loudspeaker arrays are always two-dimensional in this work (i.e., circularly curved and straight-line, delay-curved; see Fig. 2).

It is worth noting that the Multi-CBT technology applies equally well to any number of sub-CBT arrays from two on up theoretically.

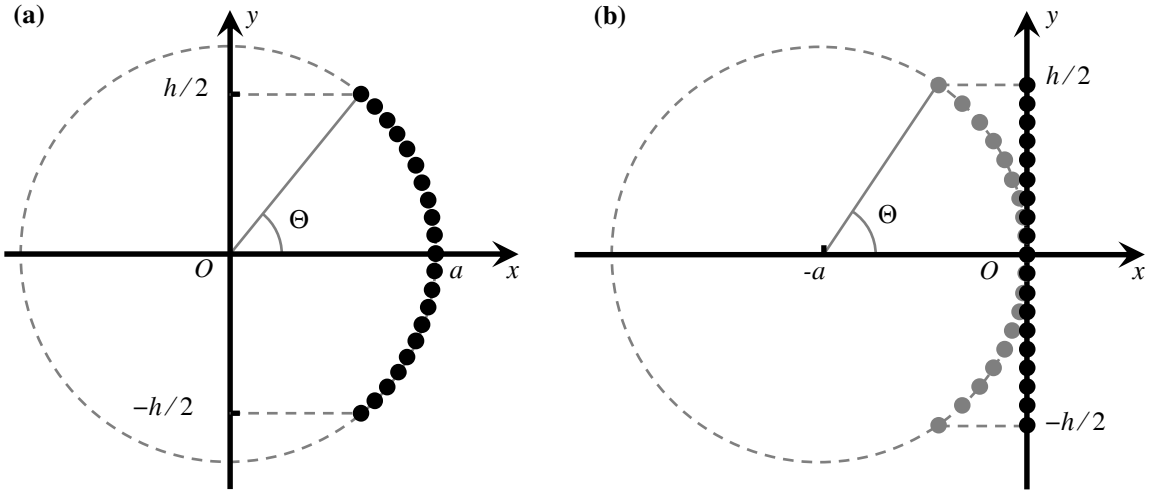

Fig. 2. **(a)** Geometry of a circularly curved multiple-source array before multiple CBT shade functions are applied to form a constant-beamwidth transducer (Multi-CBT) array. **(b)** Geometry of a straight-line, delay-curved Multi-CBT array.

3. SIMULATION

3.1. Simulation Method

In order to verify the performance of the proposed array, a simulation program similar to that described by Keele [6] is used to predict the directional characteristics of various circularly curved Multi-CBT arrays and straight-line, delay-curved Multi-CBT arrays. The following three assumptions and approximations are made in this program. (1) The array elements are regarded as omnidirectional point sources. (2) The far-field response is simulated at a distance of 250 m. (3) The Legendre function is approximated by the following equation described by Keele [6, note that the coefficient of the cubic term in the following equation was listed incorrectly as 0.743 in his paper]

$$\mathrm{P}_v(\cos\theta) \approx 1 + 0.066|x| - 1.8|x|^2 + 0.734|x|^3, \quad \text{for } |x| \le 1, \tag{5}$$

where $x = \theta / \theta_0$.

3.2. Specifications of Multi-CBT Arrays to be Simulated

In this simulation, each Multi-CBT array is chosen to consist of five sub-CBT arrays. The half-angle of each sub-CBT array is $\theta_0 = \Theta / 5$, where Θ is the (virtual) half-angle of the corresponding Multi-CBT array (see Fig. 2). The center angle of the *n*th sub-CBT array, θ_n, conforms to $\theta_n = n\theta_0 + \text{const.}$ (see Fig. 1). The specifications of the circularly curved Multi-CBT arrays and the straight-line, delay-curved Multi-CBT arrays analyzed in this work are similar to those described by Keele [6, 7] and Hawksford [1], including the parameters of array arc angle, element number, and center-to-center spacing of array elements.

3.2.1. Specifications of Circularly-Curved Multi-CBT Arrays

A broad-arc, circularly curved Multi-CBT array (arc angle of 120°) and a narrow-arc, circularly curved Multi-CBT array (arc angle of 45°) are analyzed in this work. Both arrays are designed to control vertical beamwidth over a range of 3 kHz to 20 kHz. The upper frequency limit dictates close 14 mm array-element source spacing. The lower frequency limit dictates an array height h of 1.03 m for the broad-arc 120° curved array and 2.20 m for the narrow-arc 45° curved array. To maintain the close 14 mm source spacing, the broad-arc array requires 90 point sources and the narrow-arc array requires 162 point sources. According to the previous work [6], the narrow-arc array height is supposed to be 120°/45° = 2.67 times taller than the broad-arc array height. However, the 2.20-m array can achieve similar performance using less array elements.

3.2.2. Specifications of Straight-Line, Delay-Curved Multi-CBT Arrays

A broad-virtual-arc, straight-line, delay-curved Multi-CBT array (virtual-arc angle of 90°) and a narrow-virtual-arc, straight-line, delay-curved Multi-CBT array (virtual-arc angle of 45°) are also analyzed in this work. Here, the broad virtual-arc (90°) is narrower than that of the broad-arc, circularly curved Multi-CBT array (120°), considering that the straight-line, delay-curved CBT array does not perform well when its virtual-arc is broad [7]. The array elements are equally spaced and the close 10 mm spacing ensures operation to above 20 kHz without grating lobes. The broad-virtual-arc array is composed of 138 point sources, such that the height h is 1.37 m, which ensures that the array works continuously down to 3 kHz. Similarly, more array elements are needed to ensure that the narrow-virtual-arc array works continuously down to 3 kHz (because of its narrow virtual-arc). Therefore, the narrow-virtual-arc array is composed of 210 point sources with a height h of 2.09 m. Note the height of the narrow-virtual-arc array has also been adjusted for practical reasons.

3.3. Simulation Scenarios

In order to illustrate realistic and application-oriented examples, the amplitude weights of the sub-CBT arrays are set to provide equal SPLs over a straight-line audience region, shown in Fig. 3 between points A and B.

In Fig. 3a, the broad-arc, circularly curved Multi-CBT array (arc angle of 120°) is used in this application. The first sub-CBT array aims at clockwise 10° to the vertical direction (i.e., $\theta_1 = -10°$), so that the sub-CBT arrays aim at −10°, 10°, 30°, 50°, and 70° respectively. Then the distance ratios for each sub-CBT array orientation from the nearest point (i.e., point A) to the farthest point (i.e., point B) are $1.00 : 1.00 : 1.14 : 1.53 : 2.88$. At this stage, the amplitude weights are set to be {−9.2, −9.2, −8.0, −5.5, 0.0} dB.

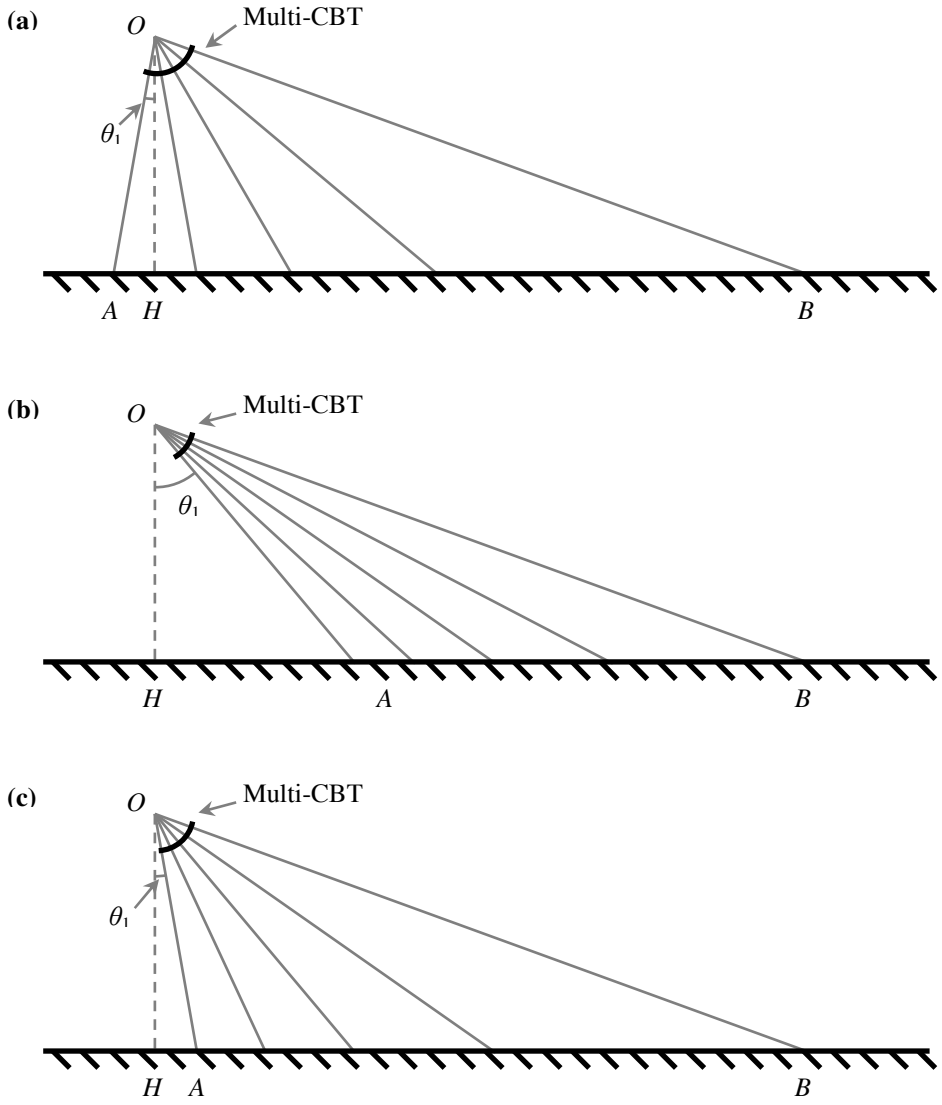

Fig. 3. Application examples of multiple constant-beamwidth transducer (Multi-CBT) arrays that provides constant SPL over a straight-line audience region from point A to B. **(a)** Broad-arc, circularly curved Multi-CBT array (arc angle of 120°); **(b)** Narrow-arc Multi-CBT array (arc angle or virtual-arc of 45°) implemented using both a circular-arc and straight-line, delay-curved arrays; **(c)** Broad-virtual-arc, straight-line, delay-curved Multi-CBT array (virtual-arc angle of 90°).

In Fig. 3b, the 45° narrow-arc Multi-CBT array is simulated using both the circular-arc and straight-line, delay-curved arrays. The first sub-CBT array aims at counter-clockwise 40° to the vertical direction (i.e., $\theta_1 = 40°$), so that the sub-CBT arrays aim at 40°, 47.5°, 55°, 62.5°, and 70° respectively. Then the distance ratios for each sub-CBT array orientation from the nearest point (i.e., point A) to the farthest point (i.e., point B) are $1.00 : 1.13 : 1.34 : 1.66 : 2.24$. At this stage, the amplitude weights are set to be {−7.0, −5.9, −4.5, −2.6, 0.0} dB.

In Fig. 3c, the broad-virtual-arc, straight-line, delay-curved Multi-CBT array (virtual-arc angle of 90°) is used in this application. The first sub-CBT array aims at counterclockwise 10° to the vertical direction (i.e., $\theta_1 = 10°$), so that the sub-CBT arrays aim at 10°, 25°, 40°, 55°, and 70° respectively. Then the distance ratios for each sub-CBT array orientation from the nearest point (i.e., point A) to the farthest point (i.e., point B) are $1.00 : 1.09 : 1.29 : 1.72 : 2.88$. At this stage, the amplitude weights are set to be {−9.2, −8.4, −7.0, −4.5, 0.0} dB.

4. RESULTS

4.1. Simulation Results of Circularly-Curved Multi-CBT Arrays

Figs. 5 - 8 illustrate the directional characteristics of the circularly curved Multi-CBT arrays. Figs. 5 and 6 apply to the broad-arc array Fig. 3a, while Figs. 7 and 8 apply to the narrow-arc array Fig. 3b.As the figures show, the circularly curved Multi-CBT arrays perform well and consistently between 3 kHz and 20 kHz, and the amplitude patterns also meet the expectations (i.e., {−9.2, −8.0, −5.5, 0.0} dB and {−7.0, −5.9, −4.5, −2.6, 0.0} dB respectively). As Figs 5a and 7a show, the correspondences between the summed Legendre functions and the simulated polar plots are quite good for both the broad-arc array and the narrow-arc array. The pressure-field plots in Figs. 6 and 8 show that the SPL distribution in the audience region is quite flat and that the SPL variance is only around ±1 dB at each frequency.

All the following pressure-field plots shown in Figs. 6, 8, 10, 12, and 14 use the color scale shown in Fig. 4.

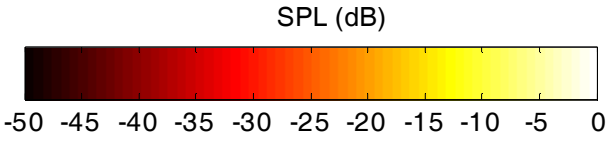

Fig. 4. Color-scale used for the pressure-field plots. Scale varies from white at 0 dB to low-level black at −50 dB in steps of 2.5 dB.

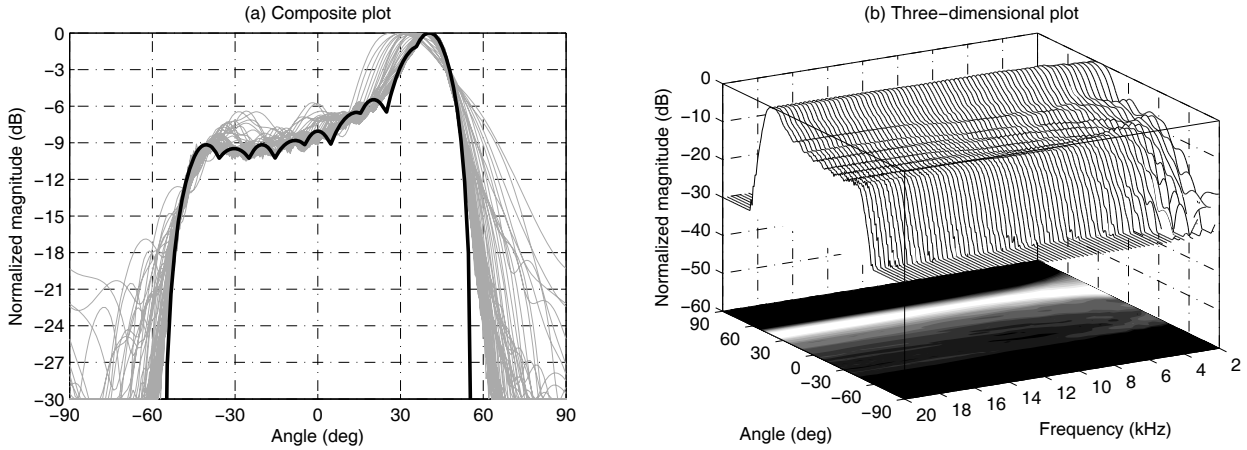

Fig. 5. Polar plots (in *x*-*O*-*y* plane) for the broad-arc, circularly curved Multi-CBT array. The angle is normalized to the center angle of the Multi-CBT and the magnitude is normalized to the max value at each frequency. **(a)** Comparison of the summed Legendre functions (black thick line) with the simulated polar plots (gray thin lines) for the broad-arc array. **(b)** Three-dimensional plot for the broad-arc array with projected two-dimensional polar plot on bottom display. Data for 73 frequencies between 2 kHz and 20 kHz are plotted with linear spacing in between.

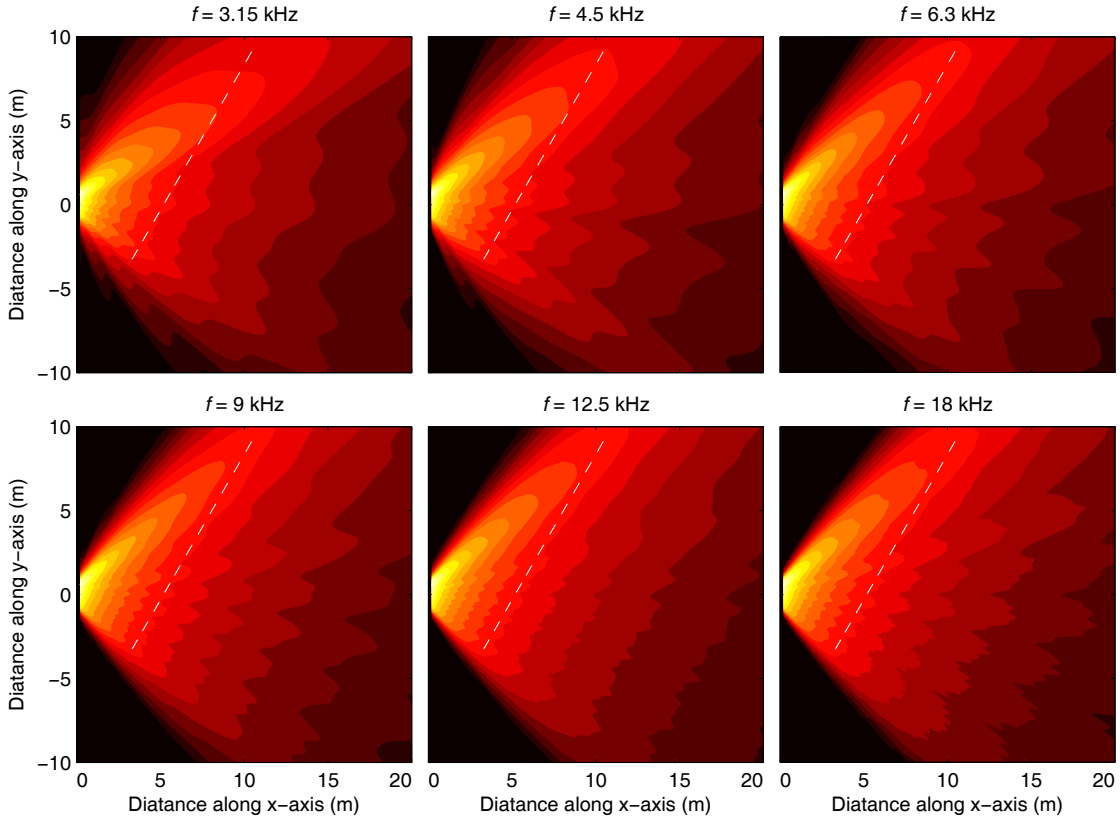

Fig. 6. Pressure fields of the broad-arc, circularly curved Multi-CBT array at different frequencies. Refer to Fig. 4 for color-scale. The dashed line indicates the audience region between points A and B, shown in Fig. 3a.

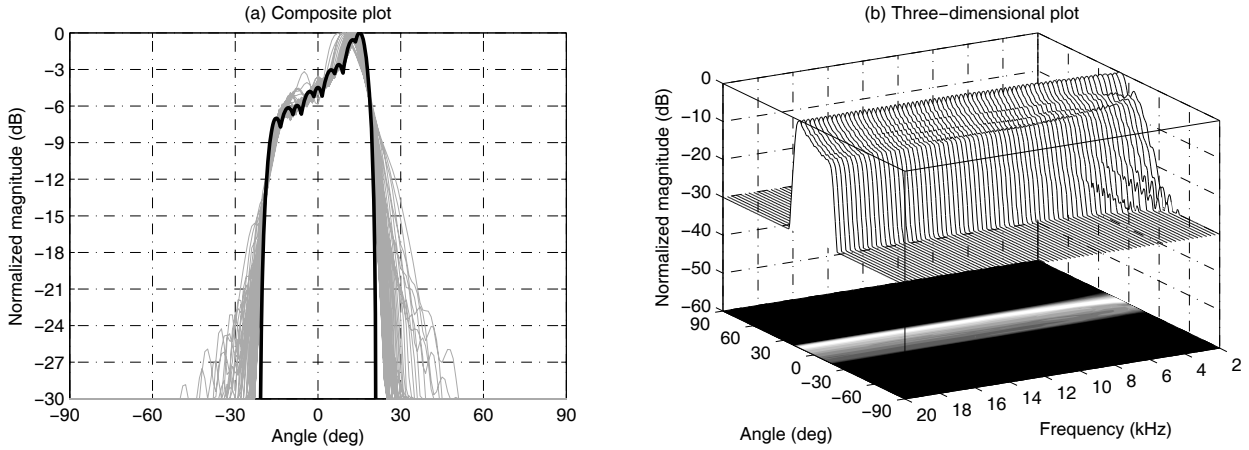

Fig. 7. Polar plots (in *x*-*O*-*y* plane) for the narrow-arc, circularly curved Multi-CBT array. This is the array that provides constant SPL over the straight audience line shown in Fig. 3. The angle is normalized to the center angle of the Multi-CBT and the magnitude is normalized to the max value at each frequency. **(a)** Comparison of the summed Legendre functions (black thick line) with the simulated polar plots (gray thin lines) for the narrow-arc array. **(b)** Three-dimensional plot for the narrow-arc array with projected two-dimensional polar plot on bottom display. Refer to Fig. 5 for information on data frequencies and spacing.

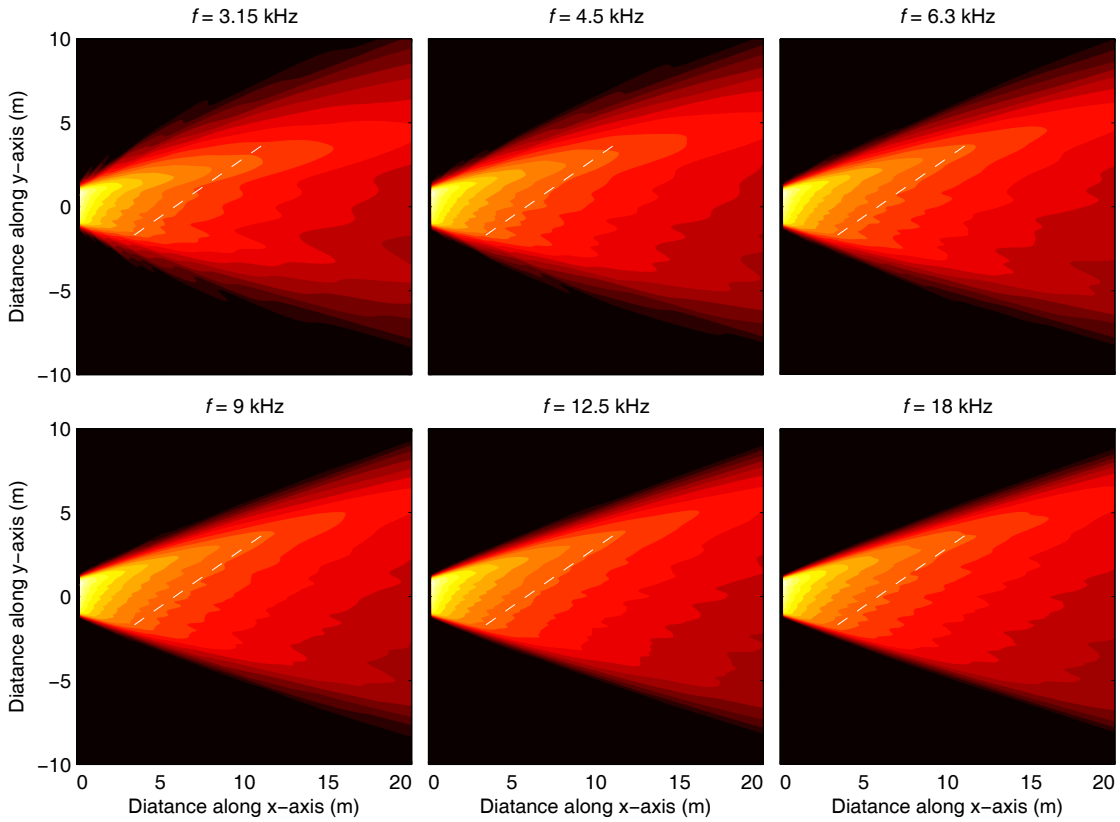

Fig. 8. Pressure fields of the narrow-arc, circularly curved Multi-CBT array at different frequencies. Refer to Fig. 4 for color-scale. The dashed line indicates the audience region between points A and B, shown in Fig. 3b.

4.2. Simulation Results of Straight-Line Delay-Curved Multi-CBT Arrays

Figs. 9 - 12 illustrate the directional characteristics of the straight-line, delay-curved Multi-CBT arrays. Figs. 9 and 10 apply to the broad-virtual -arc array, while Figs. 11 and 12 apply to the narrow-virtual-arc array.

As Figs. 9 and 10 show, some distortions are observed in the amplitude pattern of the broad-virtual-arc, straight-line, delay-curved Multi-CBT array, particularly for extreme angles and its coverage is broader than expected (see Fig. 9). As Fig. 9a shows, the correspondence between the summed Legendre functions and the simulated polar plots is not quite as good as the two previous comparisons in Figs. 5a and 7a. Additionally, as Fig 10 shows, the SPL distribution in audience region is not so flat and the SPL variance is around ±1.5 dB at each frequency. Nevertheless, the distortions are not severe, and the performance of the broad-virtual-arc array is also satisfactory (see Figs. 9 and 10). It is worth noting that the observation that the distortions exist for the broad-virtual-arc, straight-line, delay-curved array is in agreement with that described in the previous work [7]. Altogether, it is concluded that the directional characteristics of the Multi-CBT arrays are quite similar to those of the single-CBT arrays in terms of their capability to maintain a desired polar pattern shape independent of frequency [2, 6].

However, as Figs. 11 and 12 show, the performance of the narrow-virtual-arc, straight-line, delay-curved Multi-CBT array is also quite satisfactory As Fig. 11a shows, the comparison between the summed Legendre functions and the simulated polar plots is quite good as contrasted with the comparison for the broad-virtual-arc array shown in Fig. 9a. Additionally, as Fig 12 shows, similar to the circularly curved Multi-CBT arrays, the SPL distribution in audience region is also quite flat and the SPL variance is also around ±1 dB at each frequency.

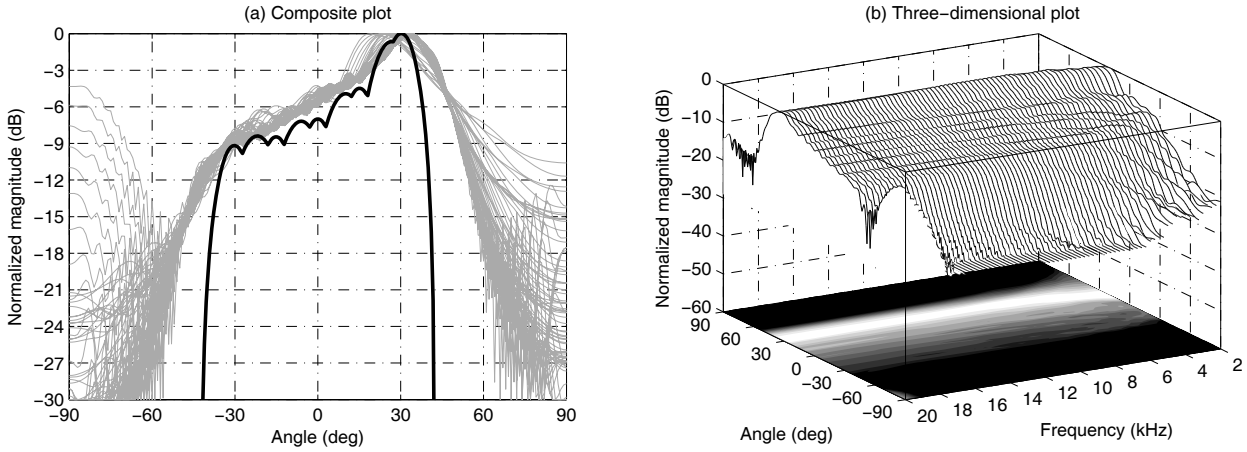

Fig. 9. Polar plots (in *x*-*O*-*y* plane) for the broad-virtual-arc, straight-line, delay-curved Multi-CBT array. The angle is normalized to the center angle of the Multi-CBT and the magnitude is normalized to the max value at each frequency. **(a)** Comparison of the summed Legendre functions (black thick line) with the simulated polar plots (gray thin lines) for the broad-virtual-arc array. **(b)** Three-dimensional plot for the broad-virtual-arc array with projected two-dimensional polar plot on bottom display. Refer to Fig. 5 for information on data frequencies and spacing.

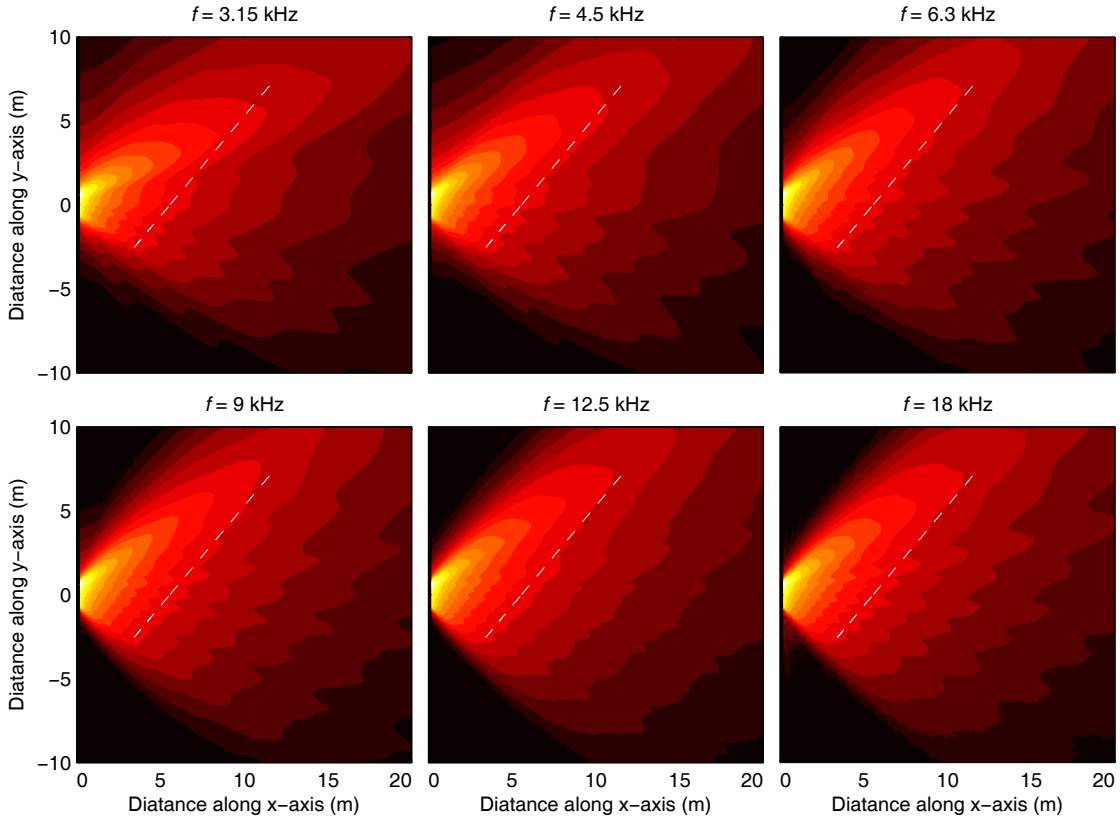

Fig. 10. Pressure fields of the broad-virtual-arc, straight-line, delay-curved Multi-CBT array at different frequencies. Refer to Fig. 4 for color-scale. The dashed line indicates the audience region between points A and B, shown in Fig. 3c.

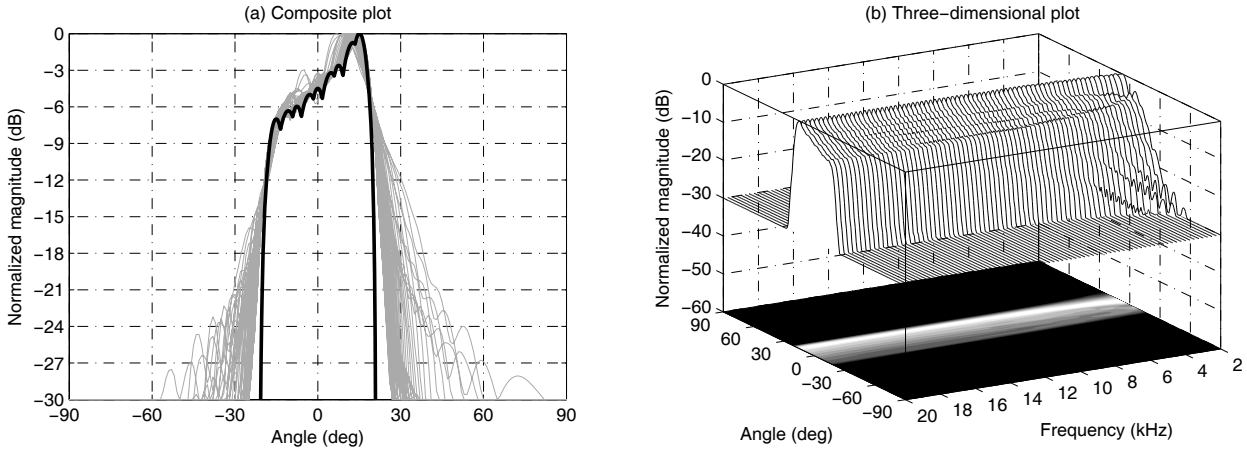

Fig. 11. Polar plots (in *x*-*O*-*y* plane) for the narrow-virtual-arc, straight-line, delay-curved Multi-CBT array. The angle is normalized to the center angle of the Multi-CBT and the magnitude is normalized to the max value at each frequency. **(a)** Comparison of the summed Legendre functions (black thick line) with the simulated polar plots (gray thin lines) for the narrow-virtual-arc array. **(b)** Three-dimensional plot for the narrow-virtual-arc array with projected two-dimensional polar plot on bottom display. Refer to Fig. 5 for information on data frequencies and spacing.

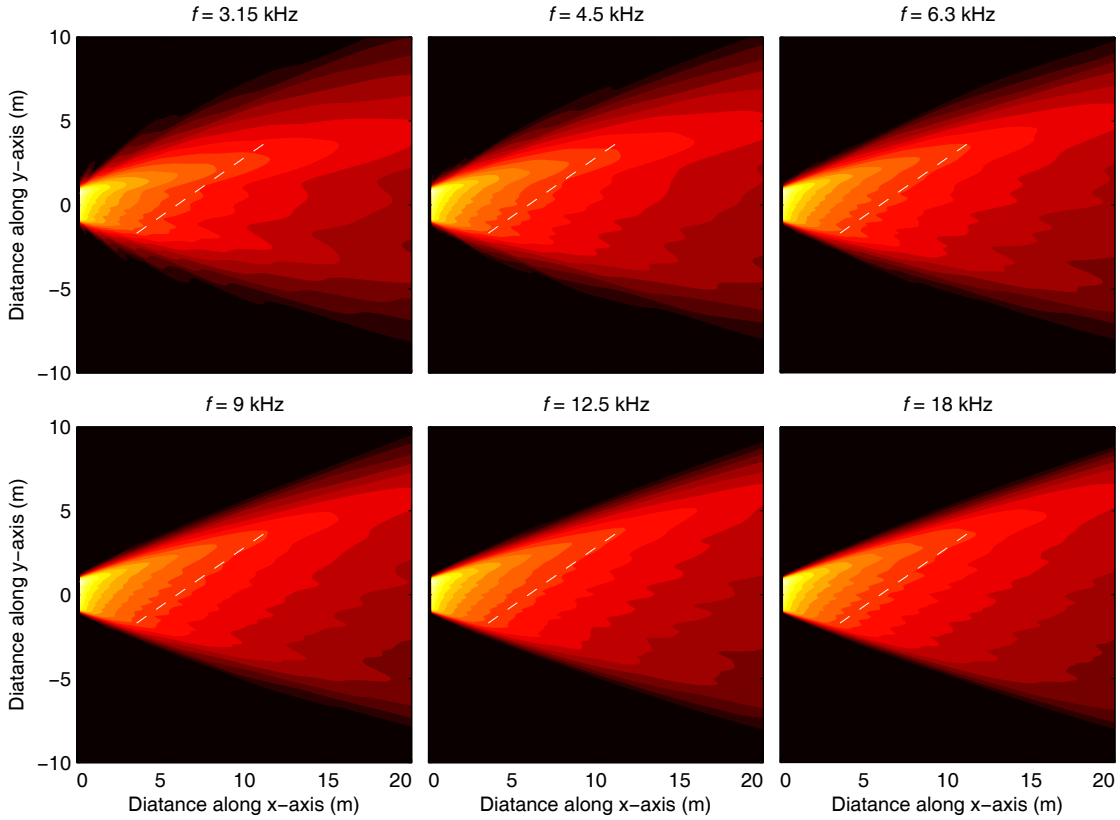

Fig. 12. Pressure fields of the narrow-virtual-arc, straight-line, delay-curved Multi-CBT array at different frequencies. Refer to Fig. 4 for color-scale. The dashed line indicates the audience region between points A and B, shown in Fig. 3b.

5. DISCUSSIONS

5.1. Improvement of Broad-Virtual-Arc, Straight-Line, Delay-Curved Multi-CBT Array

The performance of the broad-virtual-arc, straight-line, delay-curved Multi-CBT array can be improved by using more array elements with the same array height. Figs. 13 and 14 show the performance of the improved array whose element number is triple that of the original array. As the figures show, the distortions have been minimized. Note the improvement in Fig. 13a compared to Fig. 9a, particularly for extreme angles, and as Fig 14 shows, the SPL distribution in audience region has been improved and the SPL variance is around ±1 dB at each frequency. However, the exchange is obvious: more elements and smaller spacing require a higher cost and smaller transducers, and a balance between these two opposing factors should be considered. Therefore, both the cost and the performance (e.g., the operating frequency range) of the array need to be considered.

5.2. Mathematical Notes

It is also worth noting that the half-angle of each sub-CBT array is set to be 80% of the expected value in order to avoid interference between the sub-CBT arrays. This applies to all the arrays analyzed in this paper. The interference might be caused by the tiny side lobes of the sub-CBT arrays, which are thought to result from the approximation in the CBT theory. In fact, the sound pressure distribution $p(\theta)$ is not exactly zero outside the Legendre interval ($\theta > \theta_0$) as approximated in the CBT theory. Another effect caused by the approximation in the CBT theory is that the amplitudes at the sampling angles in the directivity pattern are not strictly equal to the expectation. However, the difference between the simulation and theory is minor as Figs. 5a, 7a, 9a, 11a and 13a show, indicating the good performance of the Multi-CBT array.

In essence, the Multi-CBT array is a multiple-beam array constructed by applying several overlapping CBT Legendre shading functions to an un-shaded circular-arc or a straight-line delay-curved array. The advantage is that the Multi-CBT array avoids the comb-filtering effect, which would exist in a single array that generates multiple beams steered in different directions by using electronic delays [10]. The Multi-CBT array accomplishes this by avoiding correlated signals, which are delayed by different amounts and fed to each array element.

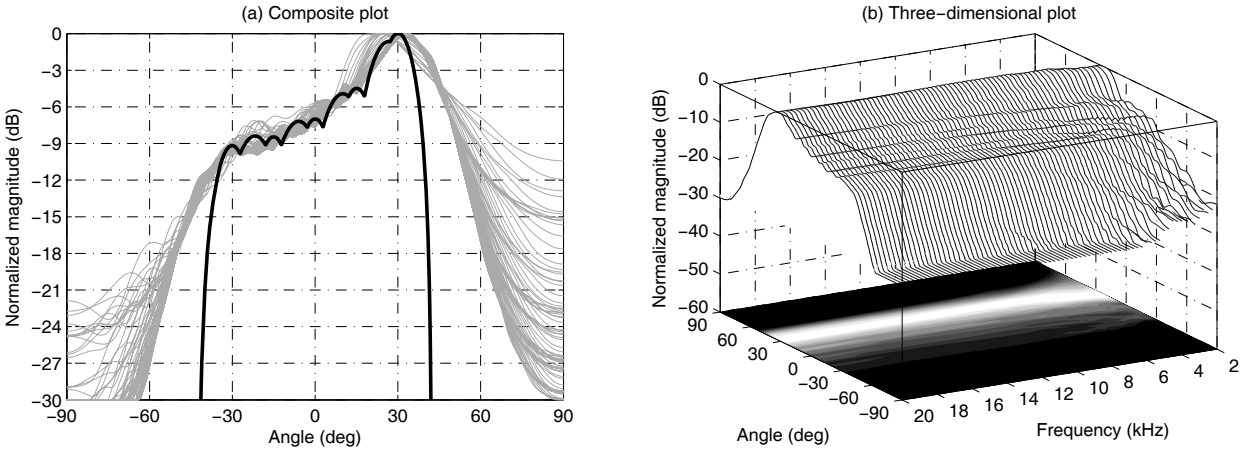

Fig. 13. Polar plots (in *x-O-y* plane) for the improved broad-virtual-arc, straight-line, delay-curved Multi-CBT array. This improved array contains triple the number of elements of the array whose results are shown in Figs. 9 and 10. The angle is normalized to the center angle of the Multi-CBT and the magnitude is normalized to the max value at each frequency. **(a)** Comparison of the summed Legendre functions (black thick line) with the simulated polar plots (gray thin lines) for the improved broad-virtual-arc array. **(b)** Three-dimensional plot for the improved broad-virtual-arc array with projected two-dimensional polar plot on bottom display. Refer to Fig. 5 for information on data frequencies and spacing.

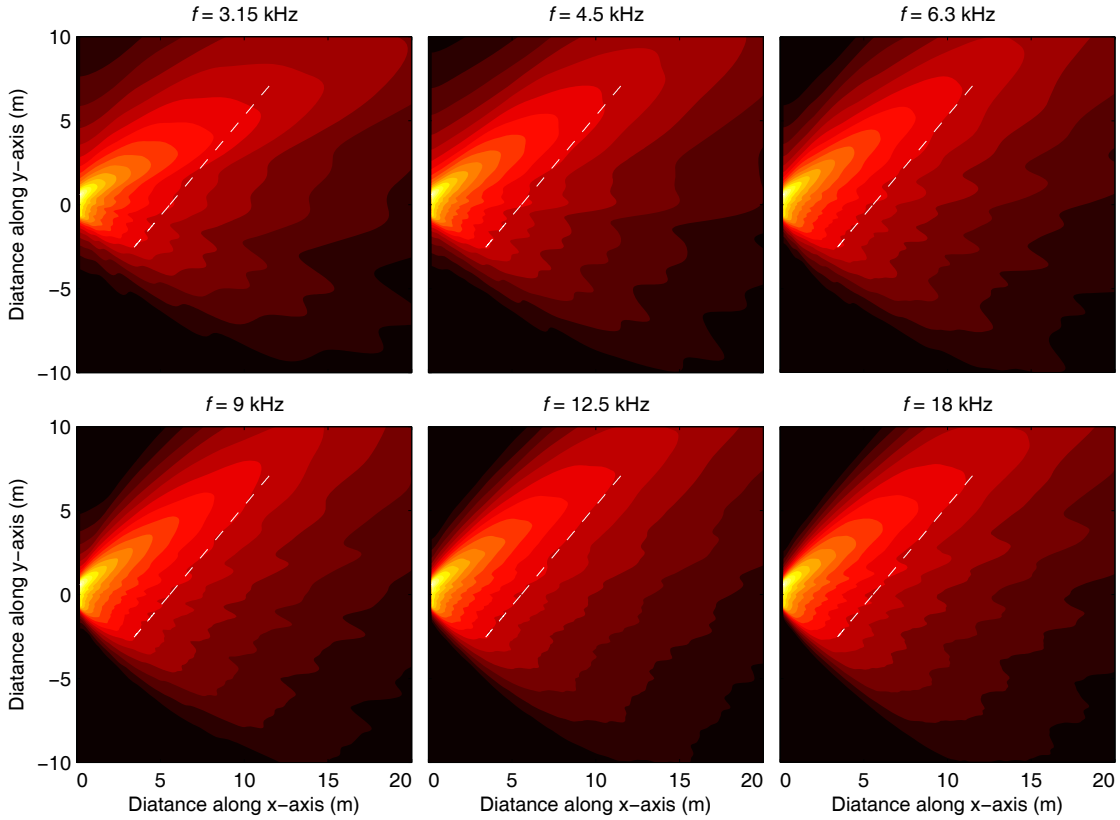

Fig. 14. Pressure fields of the improved broad-virtual-arc, straight-line, delay-curved Multi-CBT array of Fig. 13 at different frequencies. Refer to Fig. 4 for color-scale. The dashed line indicates the audience region between points A and B, shown in Fig. 3c.

5.3. Design Tips

Finally, here are some guidelines for the design of the Multi-CBT array. Generally, the height of the array is inversely proportional to the lower bandwidth limitation and the (virtual) arc angle. The estimation equations for these quantities were given by Keele [11]. Additionally, the center-to-center spacing of the array elements should be on the order of the wavelength or less at the upper operating frequency in order to avoid aliasing distortion. Once the height of the array and the center-to-center spacing of the elements are known, the element number can then be calculated.

6. SUMMARY

In summary, a Multi-CBT array can be implemented by using several overlapping CBT Legendre shading functions which are applied to an un-shaded circular-arc or a straight-line delay-curved array of acoustic sources to achieve the desired directivity pattern over a wide frequency band. The directional characteristics of various circularly curved Multi-CBT arrays and straight-line, delay-curved Multi-CBT arrays have been analyzed. The results indicate that the directional characteristics of Multi-CBT arrays are quite similar to those of single-CBT arrays in terms of their capability to maintain a desired polar pattern shape independent of frequency, and that the desired directivity patterns can be realized. An additional advantage of Multi-CBT arrays is the simplicity of allowing the shape to be specified by only a few number of real-valued weighting factors that govern the strength of the individual Legendre shading amplitudes. Since there is a strong demand for broadband directivity-customizable arrays in the fields that relate to acoustic transducers (e.g., electroacoustics), the Multi-CBT arrays have the potential for a broad range of ap-

plications, and future work will aim to realize practical implementations in acoustic transducers.

7. ACKNOWLEDGEMENTS

This work was supported by National Natural Science Foundation of China, Grant 11274172. We wish to further acknowledge the helpful comments and editorial guidance of our third author D. B. Keele, Jr. in improving the content of this paper. The idea for the Multi-CBT array was originated solely by the first two authors of this paper: Feng and Shen.

8. REFERENCES

[1] M. O. J. Hawksford, "Smart Digital Loudspeaker Arrays," *J. Audio Eng. Soc.*, vol. 51, pp. 1133-1162 (2003 Dec.).

[2] D. B. Keele, Jr., "Comments on 'Smart Digital Loudspeaker Arrays'," *J. Audio Eng. Soc.*, vol. 54, pp.1203-1214 (2006 Dec.).

[3] M. M. Goodwin, "All-Pass Linear Arrays," *J. Audio Eng. Soc.*, vol. 56, pp. 1090-1101 (2008 Dec.).

[4] P. H. Rogers and A. L. Van Buren, "New approach to a constant beamwidth transducer," *J. Acoust. Soc. Am.*, vol. 64, pp. 38-43 (1978 July).

[5] A. L. Van Buren, L. D. Luker, M. D. Jevnager, and A. C. Tims, "Experimental constant beamwidth transducer," *J. Acoust. Soc. Am.*, vol. 73, pp. 2200-2209 (1983 June).

[6] D. B. Keele, Jr., "Full-Sphere Sound Field of Constant-Beamwidth Transducer (CBT) Loudspeaker Line Arrays," *J. Audio Eng. Soc.*, vol. 51, pp. 611-624 (2003 July/Aug.).

[7] D. B. Keele, Jr., "Implementation of Straight-Line and Flat-Panel Constant Beamwidth Transducer (CBT) Loudspeaker Arrays Using Signal Delays," presented at the 113th Convention of the Audio Engineering Society, *J. Audio Eng. Soc. (Abstracts)*, vol. 50, p. 958 (2002 Nov.), Convention Paper 5653.

[8] D. B. Keele, Jr., "Practical Implementation of Constant Beamwidth Transducer (CBT) Loudspeaker Circular-Arc Line Arrays," presented at the 115th Convention of the Audio Engineering Society, *J. Audio Eng. Soc. (Abstracts)*, vol. 51, p. 1218 (2003 Dec.), Convention Paper 5863.

[9] D. B. Keele, Jr. and D. J. Button, "Ground-Plane Constant Beamwidth Transducer (CBT) Loudspeaker Circular-Arc Line Arrays," presented at the 119th Convention of the Audio Engineering Society, *J. Audio Eng. Soc. (Abstracts)*, vol. 53, p. 1227 (2005 Dec.), Convention Paper 6594.

[10] D. G. Meyer, "Multiple-Beam, Electronically Steered Line-Source Arrays for Sound-Reinforcement Applications," *J. Audio Eng. Soc.*, vol. 38, pp. 237-249 (1990 Apr.).

[11] D. B. Keele, Jr., "The Application of Broadband Constant Beamwidth Transducer (CBT) Theory to Loudspeaker Arrays," presented at the 109th Convention of the Audio Engineering Society, *J. Audio Eng. Soc. (Abstracts)*, vol. 48, pp. 1104-1105 (2000 Nov.), Preprint 5216.